

Estimating the Fractal Dimension of the S&P 500 Index using Wavelet Analysis

Erhan Bayraktar ^{*} H. Vincent Poor [†] K. Ronnie Sircar [‡]

June 2002; revised December 2003

Abstract

S&P 500 index data sampled at one-minute intervals over the course of 11.5 years (January 1989- May 2000) is analyzed, and in particular the Hurst parameter over segments of stationarity (the time period over which the Hurst parameter is almost constant) is estimated. An asymptotically unbiased and efficient estimator using the log-scale spectrum is employed. The estimator is asymptotically Gaussian and the variance of the estimate that is obtained from a data segment of N points is of order $\frac{1}{N}$. Wavelet analysis is tailor made for the high frequency data set, since it has low computational complexity due to the pyramidal algorithm for computing the detail coefficients. This estimator is robust to additive non-stationarities, and here it is shown to exhibit some degree of robustness to multiplicative non-stationarities, such as seasonalities and volatility persistence, as well. This analysis shows that the market became more efficient in the period 1997-2000.

^{*}Department of Electrical Engineering, Princeton University, E-Quad, Princeton, NJ 08544, ebayrak@ee.princeton.edu

[†]Department of Electrical Engineering, Princeton University, E-Quad, Princeton, NJ 08544, poor@ee.princeton.edu

[‡]Department of Operations Research & Financial Engineering, Princeton University, E-Quad, Princeton, NJ 08544, sircar@princeton.edu

¹2000 Mathematics Subject Classification. 91B82, 91B84, 60G18, 60G15, 65T60

²**Key Words:** High-frequency data, S&P 500 index, long range dependence, heavy tailed marginals, fractional Brownian motion, wavelet analysis, log scale spectrum

1 Introduction

Stochastic models based primarily on continuous or discrete time random walks have been the foundation of financial engineering since they were introduced in the economics literature in the 1960s. Such models exploded in popularity because of the successful option pricing theory built around them by Black and Scholes [13] and Cox *et al.* [15], as well as the simplicity of the solution of associated optimal investment problems given by Merton [33].

Typically, models used in finance are diffusions built on standard Brownian motion and they are associated with partial differential equations describing corresponding optimal investment or pricing strategies. At the same time, the failure of models based on independent increments to describe certain financial data has been observed since Greene and Fielitz [21] and Mandelbrot [31], and [30]. Using R/S analysis, Greene and Fielitz studied 200 daily stock returns of securities listed on the New York Stock Exchange and they found significant long range dependence. Contrary to their finding, Lo [27], using a modified R/S analysis designed to compensate for the presence of short-range dependence, finds no evidence of long-range dependence (LRD). However, Teverovsky *et al.* [46] and Willinger *et al.* [47] identified a number of problems associated with Lo's method. In particular, they showed that Lo's method has a strong preference for accepting the null hypothesis of no long range dependence. This happens even with long-range dependent synthetic data. To account for the long-range dependence observed in financial data Cutland *et al.* [16] proposed to replace Brownian motion with *fractional Brownian motion* (fBm) as the building block of stochastic models for asset prices. An account of the historical development of these ideas can be traced from Cutland *et al.* [16], Mandelbrot [32] and Shiryaev [43]. The S&P 500 index was analyzed in [37] and [38] by Peters using R/S analysis, and he concluded that the raw return series exhibits long-range dependence. See also [24] for analysis of LRD in German stock indices.

Here we present a study of a high-frequency financial data set exhibiting long-range dependence, and develop wavelet based techniques for its analysis. In particular we examine the S&P 500 over 11.5 years, taken at one-minute intervals. The wavelet tool we consider, namely the log-scale spectrum method, is asymptotically unbiased and efficient with a vanishing precision error for estimating the Hurst parameter (a measure of long-range dependence, explained in (2) below). (See Theorem 2.1.) Since we are dealing with high frequency data, we need fast algorithms for the processing of the data. Wavelet analysis is tailor-made for this purpose due to the pyramidal algorithm, which calculates the wavelet coefficients using octave filter banks. In essence, we look at a linear transform of the logarithm of the wavelet variance (*i.e.* the variance of the detail coefficients, defined in (9)) to estimate the Hurst parameter. Moreover, the log-scale spectrum methodology is insensitive to additive non-stationarities, and, as we shall see, it also exhibits robustness to multiplicative non-stationarities of a very general type including seasonalities and volatility persistence (Section 2.4).

Although the Hurst parameter of S&P 500 data considered here is significantly above the efficient market value of $H = \frac{1}{2}$, it began to approach that level around 1997. This behavior of the market might be related to the increase in Internet trading, which has the three-fold effect of increasing the number of small traders, increasing the frequency of trading activity, and improving traders' access to price information. An analytical model of this observation is proposed in [10].

1.1 Fractional Brownian Motion

A natural extension of the conventional stochastic models for security prices to incorporate long-range dependence is to model the price series with geometric fractional Brownian motion:

$$P_t = P_0 \exp \left(\mu t + \int_0^t \sigma_s dB_s^H \right), \quad (1)$$

where P_0 is today's observed price, μ is a growth rate parameter, σ is the stochastic volatility process, and B^H is a fractional Brownian motion, an almost surely (a.s.) continuous and centered Gaussian process with stationary increments. autocorrelation of B^H

$$\mathbb{E} \{ B_t^H B_s^H \} = \frac{1}{2} (|t|^{2H} + |s|^{2H} - |t-s|^{2H}), \quad (2)$$

where $H \in (0, 1]$ is the so-called Hurst parameter. (Note that $H = \frac{1}{2}$ gives standard Brownian motion.) From this definition, it is easy to see that fBm is self-similar, *i.e.* $B^H(at) = a^H B(t)$, where the equality is in the sense of finite dimensional distributions. This model for stock market prices is a generalization of the model proposed in [16] to allow for non-Gaussian returns distribution into the model. Heavy tailed marginals for stock price returns have been observed in many empirical studies since the early 1960's by Fama [20] and Mandelbrot [29].

Fractional Brownian motion models are able to capture long range dependence in a parsimonious way. Consider for example the fractional Gaussian noise $Z(k) := B^H(k) - B^H(k-1)$. The auto-correlation function of Z , which is denoted by r , satisfies the asymptotic relation

$$r(k) \sim r(0)H(2H-1)k^{2H-2}, \quad \text{as } k \rightarrow \infty. \quad (3)$$

For $H \in (1/2, 1]$, Z exhibits long-range dependence, which is also called the Joseph effect in Mandelbrot's terminology [32]. For $H = 1/2$ all correlations at non-zero lags are zero. For $H \in (0, 1/2)$ the correlations are summable, and in fact they sum up to zero. The latter case is less interesting for financial applications ([16]).

Now, we will make the meaning of (1) clear by defining the integral term. The stochastic integral in (1) is understood as the probabilistic limits of Stieltjes sums. That is, given stochastic processes Y and X , such that Y is adapted to the filtration generated by X , we say that the integral $\int Y dX$ exists if, for every $t < \infty$, and for each sequence of partitions $\{\sigma^n\}_{n \in \mathbb{N}}$, $\sigma^n = (T_1^n, T_2^n, \dots, T_{k_n}^n)$, of the interval $[0, t]$ that satisfies $\lim_{n \rightarrow \infty} \max_i |T_{i+1}^n - T_i^n| = 0$, the sequence of sums $\left(\sum_i Y_{T_i^n} (X_{T_{i+1}^n} - X_{T_i^n}) \right)$ converges in probability. That is, we define

$$\int_0^t Y_s dX_s = \mathbb{P} - \lim_{n \rightarrow \infty} \sum_i Y_{T_i^n} (X_{T_{i+1}^n} - X_{T_i^n}). \quad (4)$$

By the Bichteler-Dellacherie Theorem [39] one can see that the integrals of adapted processes with respect to fBm may not converge in probability. However when $H > \frac{1}{2}$ there are two families of processes that are integrable with respect to fBm that are sufficiently large for modeling purposes. The first family consists of continuous semi-martingales adapted to the filtration of fBm as demonstrated in [8]. The second family consists of processes with Hölder exponents greater than $1 - H$. (This integration can be carried out pathwise as demonstrated in [41], and [48]).

1.2 Markets with Arbitrage Opportunities

Much of finance theory relies on the assumption that markets adjust prices rapidly to exclude any arbitrage opportunities. It is well known that models based on fBm allow arbitrage opportunities ([14] and [40]). Even in the case of stochastic σ we have shown that there exist arbitrage opportunities in a single stock setting [8]. However, strategies that capitalize on the smoothness (relative to standard Bm) and correlation structure of fBm to make gains with no risk, involve exploiting the fine-scale properties of the process' trajectories. Therefore, this kind of model describes a market where arbitrage opportunities can be realized (by frequent trading), which seems plausible in real markets. But the ability of a trader to implement this type of strategy is likely to be hindered by market frictions, such as transaction costs and the minimal amount of time between two consecutive transactions. Indeed Cheridito [14] showed that by introducing a minimal amount of time $h > 0$ between any two consecutive transactions, arbitrage opportunities can be excluded from a geometric fractional Brownian motion model (*i.e* when σ is taken to be constant in (1)).

Elliot and Van der Hoek [19], and Oksendal and Hu [35] considered another fractional Black-Scholes (B-S) model by defining the integrals in (1) as Wick type integrals. This fractional B-S model does not lead to arbitrage opportunities; however one can argue that it is not a suitable model for stock price dynamics. The Wick type integral of a process Y with respect to a process X is defined as

$$\int_0^t Y_{T_i^n} \diamond (X_{T_{i+1}^n} - X_{T_i^n}) \quad (5)$$

where the convergence is in the L^2 space of random variables. (The Wick product is defined using the tensor product structure of L^2 ; see [25].) The Wick type integral of Y with respect to fBm with Hurst parameter H is equal to the Stieltjes integral defined above plus a drift term (see [18] Thm. 3.12),

$$\int_0^t Y_s dB_s^H = \int_0^t Y_s \diamond dB_s^H + \int_0^t D_s^\phi Y_s ds,$$

where $\phi(s, t) = H(2H - 1)|s - t|^{2H-2}$, and $D_s^\phi Y_t := (D^\phi Y_t)(s)$ is the Hida derivative of the random variable Y_t . Hence writing an integral equation in terms of Wick product integrals is equivalent to writing a Stieltjes differential equation with a different drift term. The fractional B-S model with the integrals defined as in (5) does not lead to arbitrage opportunities. However, this conclusion is based on the redefinition of the class of self-financing strategies. The self-financing strategies in a Stieltjes framework are no longer self-financing strategies in a Wick framework, so that all the self-financing arbitrage strategies of the Stieltjes framework are ruled out by the approach of [19] and [35]. However in the Wick framework it is hard to give economic interpretations to trading strategies. For illustration let us consider a simple hold strategy. Let u denote the number of shares that are held at time T_1 by an economic agent, and let us see the value change of the portfolio over the time interval $[T_1, T_2]$ if the agent chooses to hold its shares of the risky asset in a Wick type framework. If P_t denotes the price of the risky asset at time t , the increment of the value of the portfolio over the interval $[T_1, T_2]$ is

$$u \diamond (P_{T_2} - P_{T_1}). \quad (6)$$

It is hard to attach a clear economic meaning to this quantity since the Wick product is not a path-wise product but rather is defined using the tensor product structure of the L^2 space of random variables. On the other hand, (4) involves the actual realization of the increment,

$$u(\omega)(P_{T_2}(\omega) - P_{T_1}(\omega)), \quad (7)$$

which has a clear economic interpretation. (Here, ω denotes the point in the sample space corresponding to the given realization of the price process.) So, among the two candidates for the value of the increment of a simple hold strategy, (7) has a more direct economic meaning. Hence the no arbitrage conclusion of [19] and [35] cannot be interpreted within the usual meaning of this term, and thus we prefer to apply the definition (4) for the stochastic integrals involved. (Also see [12] and [44] which also argue that Wick type integrals are not suitable for defining trading strategies.)

Models with fBm differentials in the stochastic differential equations describing the stock price can be built however, by considering the Nash-equilibrium which arises from a game in which the players are institutional investors manipulating the coefficients of a stochastic differential equation with fBm differentials in order to maximize their utilities. The Nash-equilibrium for such stochastic differential games is considered by Bayraktar and Poor in [9]. The fBm differentials in the controlled stochastic differential game can be interpreted as the trading noise arising from the activities of small investors who exhibit inertia (see [10]).

1.3 Non-stationarities Expected from a Financial Time Series

1.3.1 Time-Variation of H

In this paper, we are interested in the estimation of the Hurst parameter (H) from historical stock index data. In addition, we will study the variability of this parameter over time. Common experience with financial data suggests that it exhibits too much complexity to be described by a model as simple as (1), which says that the log price process

$$Y_t := \log(P_t/P_0) = \mu_t + \int_0^t \sigma_s dB_s^H, \quad t \in [0, T], \quad (8)$$

is a stochastic integral with respect to fBm with drift. In particular, if we could remove the non-stationarities due to the drift and stochastic volatility, then Y_t would be a process with stationary increments. However, stationarity is not usually a property of return series of a financial index, which are often extremely turbulent. Therefore, we would like to identify segments of time over which the return series is close to stationary. In other words, one of our aims is to study the variation of H over time as a gauge of the epochs when the returns process behaves like a stationary process. We do not assume any particular form of temporal behavior for this parameter; its variation is to be found from our data analysis. We partition the data into smaller segments, find the corresponding parameters for each of the segments, and use filtering to remove the extrinsic variation in the parameters due to finiteness of the segment. We vary the segmentation size and repeat the procedure described. Then, comparing the fluctuations of H among different segmentation levels, we are able to come up with the segments of stationarity. The comparison among the different levels of segmentation is possible since extra noise introduced by altering the segmentation level is filtered out. In Section 5, we show how we come to the conclusion that the segments of stationarity for the S&P 500 are on the order of 2^{14} points, or approximately 8 weeks.

1.3.2 Drift and Stochastic Volatility

We can also allow the average growth rate μ in (1) to have time variation. Our analysis is insensitive to polynomial trends of certain order. Our method, based on the analysis of the log-scale spectrum, is also insensitive to additive periodic components. The effects of periodicity on the scale spectrum, and a technique for alleviating the polluting effects of additive periodicity by increasing the number of vanishing moments of a mother wavelet is analyzed by Abry *et al.* [1] on fBm with $H = 0.8$ and an additive sinusoidal trend.

Here we are interested in S&P 500 data, for which the returns have a multiplicative periodic component and stochastic volatility in addition to their intrinsic random variation. The existence of seasonalities is observed in various financial time series: see [7] for a single stock return series, [22] for S&P 500 index data, and [4] and [5] for FEX data. Heavy tailed marginals for stock price returns have been observed in many empirical studies since the early 1960's (e.g., [21],[29]). So we expect to have stochastic volatility¹ in (1) as well. Therefore we must take into account these non-stationarities in the data while developing an estimation procedure. One way of dealing with seasonalities is given in [3] and [23]. Here we show that the scale spectrum method is quite insensitive to multiplicative nonstationarities as well as to volatility persistence.

The remainder of this paper is organized as follows. In Section 2, we introduce our estimation technique and discuss its statistical and robustness properties. In Section 3 we apply our technique to S&P 500 index data and discuss our observations.

2 The Log-Scale Spectrum Methodology

In the Appendix we provide a brief introduction to wavelets (following the treatment by Mallat [28]), and the pyramidal algorithm and its initialization. Henceforth we will assume the notation introduced in Section A.1.

For $(j, k) \in \mathbb{Z}^2$ let $d_j(k)$ denote the detail coefficient at scale j and shift k of a random process Z :

$$d_j(k) = 2^{-j/2} \int_{-\infty}^{+\infty} \psi(2^{-j}t - k)Z(t) dt, \quad (9)$$

where ψ is any function satisfying the vanishing moments condition (Appendix A.1.1, (27)) for some $p \in \mathbb{Z}_+$.

The empirical variance as a function of the scale parameter $j \in \mathbb{Z}$ is called the scale spectrum and is given by

$$S_j = \frac{1}{N/2^j} \sum_{k=1}^{N/2^j} [d_j(k)]^2, \quad j \leq \log_2(N), \quad (10)$$

where N is the number of initial approximation coefficients, i.e. for $j = 0$.

¹Observe, however, that equation (1) should not be read in the same way as financial models driven by standard Brownian motion, since the stochastic integral $\int \sigma dB^H$ is not a martingale. Moreover, σ^2 is not the quadratic variation process of this integral, and should not be viewed as the volatility process literally.

2.1 Scale Spectra and fBm

The detail coefficients of fBm satisfy the following,

$$\mathbb{E}\{[d_j(k)]^2\} = K(H)2^{(2H+1)j}, \quad (11)$$

where $K(H)$ is given by

$$K(H) = \frac{1 - 2^{-2H}}{(2H + 1)(2H + 2)}, \quad (12)$$

as given in [2], for example. The behavior in (11) suggests that the empirical variance of the sequence $(d_j(k))_{k \leq N/2^j}$ can be used to estimate the Hurst parameter H . The empirical variance of fBm satisfies

$$\mathbb{E}\{S_j\} = \mathbb{E}\{[d_j(k)]^2\} = K(H)\sigma^2 2^{(2H+1)j}.$$

We immediately see that the slope of the log scale spectrum $\log(S_j)$ yields a simple estimator of the Hurst parameter, but as we shall see one can do better than this simple estimator.

2.2 Synthetically Generated fBm and Corresponding Log-scale Spectra

In this section, we illustrate the behavior of the log-spectrum on synthetic data. We use the method of Abry and Sellan [2] to generate a realization of 2^{19} points of fBm with $H = 0.6$. This method uses wavelets for the synthesis of fBm and requires the specification of the number of scales, which we choose to be 20. This simulation method is extremely fast, which is important for our purposes since we need on the order of 1 million data points to carry out our synthetic analysis.

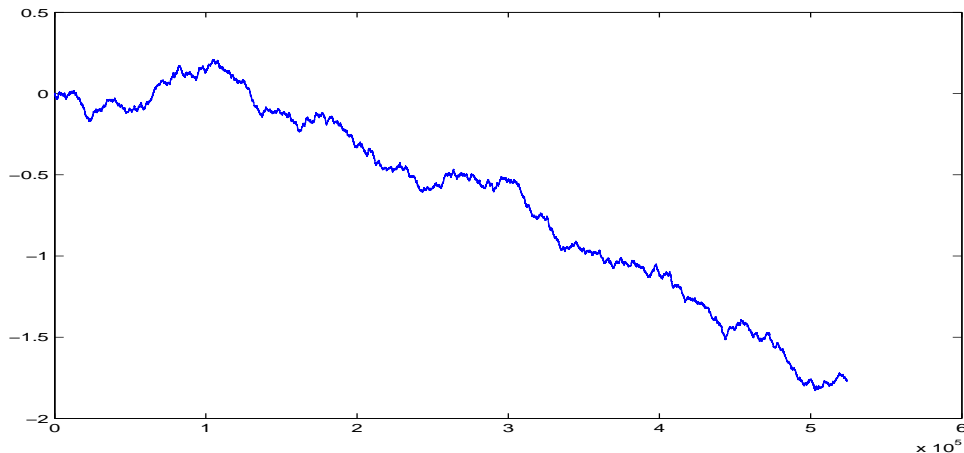


Figure 1: A realization of fBm ($H = 0.6$) of 2^{19} points created using 20 scales

We use segments of length 2^{15} (*i.e.*, 2^{15} minutes), and the estimates of the Hurst parameter over each segment for the case of fBm are shown in Fig. 3. The associated log-scale spectra are shown in Fig. 2. (The mean of the estimates of H over the segments is 0.5928, and the standard deviation(std) is 0.0149.)

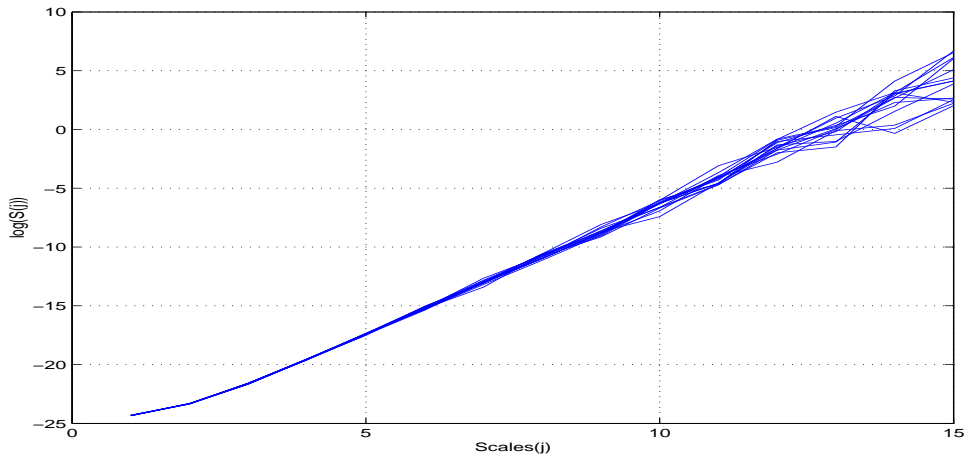


Figure 2: Log-scale spectra for segments of length 2^{15} for the realization of fBm in Fig. 1

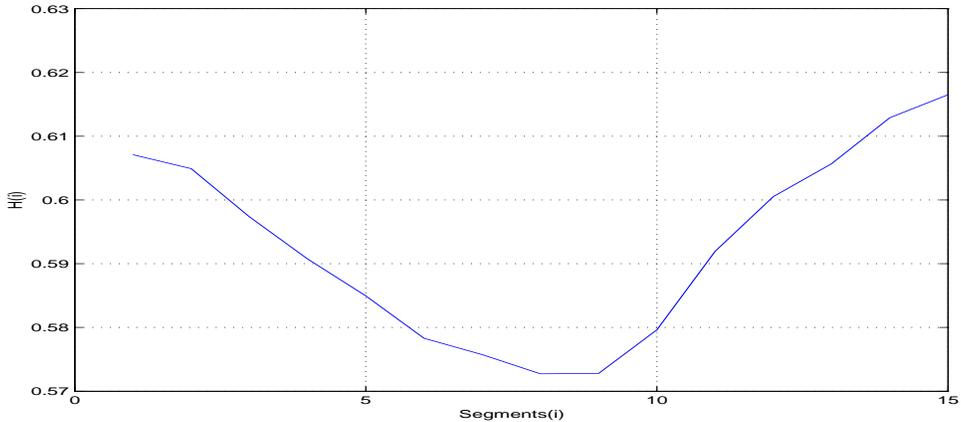


Figure 3: Hurst estimates for the realization of fBm given in Fig. 1 when the segment lengths are 2^{15}

In the next section, we will analyze the asymptotic properties of the logarithm of the scale spectrum when σ in (8) is taken to be constant, and we will develop an asymptotically efficient estimator using these results. Then in the following section, using the path properties of the integrals with respect to fBm, we will discuss the robustness of this estimator to stochastic volatility and seasonalities.

2.3 Asymptotic Distribution of the Logarithm of the Scale Spectrum

We generalize the method developed by Papanicolaou and Solna [36] to our case when the process to be analyzed is given by (8) with σ constant. The treatment of [36] was concerned with Kolmogorov turbulence for which H is around $\frac{1}{3}$, and therefore the use of a Haar wavelet in (9) suffices. In the S&P 500 data, H is expected to be greater than or equal to $\frac{1}{2}$. Below we show that for any $H \in (0,1)$ using any function ψ with two vanishing moments in (9) is

sufficient for obtaining an asymptotically Gaussian wavelet variance series (10).

Theorem 2.1 *Assume that Z in (9) is given by (8), with $\mu = 0$ and σ constant, and the analyzing wavelet in (9) has compact support and has vanishing moments of order at least 2. Then the logarithm of the scale spectrum (10), i.e. $\log_2(S_j)$, is asymptotically normally distributed and satisfies the following asymptotic relation (as $N \rightarrow \infty$):*

$$\log_2 S_j \sim \log_2(\sigma^2 K(H)) + j(2H + 1) + \frac{\epsilon_j}{\sqrt{N_j} \ln(2)} \quad j = 1, \dots, \log_2(N) \quad (13)$$

where $N_j = N/2^j$, $K(H)$ is given by (12), ϵ_j is $\mathcal{N}(0, 1)$ and

$$\text{cov} \left(\frac{\epsilon_j}{\sqrt{N_j}}, \frac{\epsilon_i}{\sqrt{N_i}} \right) \sim \frac{1}{\sqrt{N_j N_i}}, \quad (14)$$

as $N \rightarrow \infty$.

First we will state a central limit theorem for heteroskedastic random variables:

Lemma 2.1 (Berry-Essen Theorem (see [45])) *Suppose y_1, y_2, \dots, y_n are independent random variables such that*

$$\mathbb{E}\{y_i\} = 0, \quad \mathbb{E}\{y_i^2\} = \sigma_i^2 \quad \text{and} \quad \mathbb{E}\{|y_i^3|\} = \rho_i,$$

and define

$$s_n^2 = \sum_{i=1}^n \sigma_i^2 \quad \text{and} \quad r_n = \sum_{i=1}^n \rho_i.$$

Let F_n denote the distribution function of the normalized sum $\sum_{i=1}^n y_i/s_n$. Then

$$|F_n(x) - \Phi(x)| \leq 6 \frac{r_n}{s_n^3},$$

where Φ denotes the $\mathcal{N}(0, 1)$ distribution function.

Proof of Theorem 2.1:

First we will use the Berry-Essen Theorem to show that S_j given by (10) is asymptotically normal ($N \rightarrow \infty$) with mean proportional to $2^{j(2H+1)}$. Let $N_j = N/2^j$, and denote the vector of scale coefficients at scale j by $d^j = [d_j(1), \dots, d_j(N_j)]^T$. Also denote the covariance matrix of d^j by C . Note that d^j has the same law as $C^{1/2}\eta$, where η is a vector of independent $\mathcal{N}(0, 1)$ random variables. Let A be the matrix that diagonalizes C , i.e. $A^T C A = \Lambda$, where Λ is the matrix of eigenvalues of C . Since $\xi = A\eta$ has the same distribution as η , we have

$$N_j S_j = d^{jT} d^j \stackrel{d}{=} \eta^T C \eta \stackrel{d}{=} \xi^T \Lambda \xi = \sum_i \lambda_i \xi_i^2.$$

On denoting $\tilde{\Lambda} = \Lambda/\mathbb{E}\{S_j\}$, we have

$$S_j = \mathbb{E}\{S_j\} \left(1 + \frac{1}{N_j} \sum_{i=1}^{N_j} \tilde{\lambda}_i (\xi_i^2 - 1) \right).$$

Define

$$X_j = \frac{1}{N_j} \sum_{i=1}^{N_j} y_i$$

where $y_i = \tilde{\lambda}_i(\xi_i^2 - 1)$. The y_i 's are independent random variables with the following properties:

$$\mathbb{E}\{y_i\} = 0, \quad \mathbb{E}\{y_i^2\} = 2\tilde{\lambda}_i^2 \quad \text{end} \quad \mathbb{E}\{|y_i^3|\} \leq 28\tilde{\lambda}_i^3,$$

which are easily derived from the fact that the moments of a $\mathcal{N}(0, \sigma^2)$ random variable are given by the following expression:

$$\mu_j = \left(\frac{\sigma^2}{2}\right)^{j/2} \frac{j!}{\frac{j!}{2}}, \quad \text{for } j \text{ even,}$$

and the odd moments are zero. By the Berry-Essen Theorem, it is sufficient to show that

$$J = \frac{\sum_{i=1}^{N_j} \tilde{\lambda}_i^3}{[\sum_{i=1}^{N_j} \tilde{\lambda}_i^2]^{3/2}},$$

is small for large N_j . We first analyze the denominator.

$$\sum_{i=1}^{N_j} \tilde{\lambda}_i^2 = \frac{\sum_{n,m} (C_{nm})^2}{(\mathbb{E}\{S_j\})^2} = \frac{N_j}{2} \left(\frac{4}{N_j} \sum_{k=0}^{N_j-1} (N_j - k)[\rho(k)]^2 - 2 \right)$$

where

$$\rho(k) = \frac{\mathbb{E}\{d_j(n)d_j(n-k)\}}{\mathbb{E}\{[d_j(n)]^2\}}.$$

Let us introduce

$$l(H) = \lim_{N_j \rightarrow \infty} \left(\frac{4}{N_j} \sum_{k=0}^{N_j-1} (N_j - k)\rho(k)^2 - 2 \right).$$

We will now show that $\rho(k)$ decays as k^{-2p+2H} (so that $l(H)$ is a constant), where p is the number of vanishing moments and H is the Hurst exponent of the fBm. We can write

$$\mathbb{E}\{d_j(n)d_j(n-k)\} = 2^{-j}\sigma^2 \mathbb{E}\left\{ \int dx \int dt \psi_{j,n}(x)\psi_{j,n-k}(t) B^H(x)B^H(t) \right\}.$$

By (2) and Fubini's Theorem we have

$$\mathbb{E}\{d_j(n)d_j(n-k)\} = 2^{-j-1}\sigma^2 \int dx \int dt \psi_{j,n}(x)\psi_{j,n-k}(t) (|t|^{2H} + |x|^{2H} - 2|t-x|^{2H}),$$

and since $\int \psi_{j,k}(x) dx = 0$ for all (k, j) then we have

$$\begin{aligned} \mathbb{E}\{d_j(n)d_j(n-k)\} &= -2^{-j}\sigma^2 \int dx \int dt \psi_{j,n}(x)\psi_{j,n-k}(t) |t-x|^{2H} \\ &= -2^{j(2H+1)}\sigma^2 \int dt \int dx \psi(t)\psi(x) |t-x+k|^{2H}. \end{aligned} \tag{15}$$

Using Taylor's formula we have,

$$\begin{aligned} \left(1 + \frac{t-x}{k}\right)^{2H} &= 1 + \sum_{q=1}^{2p-1} \frac{\Gamma(2H+1)}{\Gamma(2H-q+1)\Gamma(q+1)} \left(\frac{t-x}{k}\right)^q \\ &\quad + \frac{\Gamma(2H+1)}{\Gamma(2H-p+1)\Gamma(p+1)} \theta(t,x,k) \left(\frac{t-x}{k}\right)^{2p}, \end{aligned} \quad (16)$$

where $\theta(t,x,k) < (1+a/k)$ and where a is the support length of the analyzing wavelet. Using (15) and the facts that the mother wavelet ψ has vanishing moments of order p and is compactly supported, we conclude that $\rho(k)$ decays as k^{-2p+2H} . (In (16), Γ denotes the gamma function.) Therefore,

$$l(H) = \lim_{N_j \rightarrow \infty} \left(\frac{4}{N_j} \sum_{k=0}^{N_j-1} (N_j - k) \rho(k)^2 - 2 \right)$$

is constant if $p \geq 2$. (Note that for any self-similar stationary increment processes with self-similarity parameter H , i.e. $X(at) \stackrel{d}{=} a^H X(t)$, for any $a > 0$, H must be in $(0,1]$; see [42].) Therefore having wavelets of vanishing moments of order 2 is necessary to cover the range $(0,1]$ for the Hurst parameter. Note that Haar (having $p = 1$) wavelets would work only for $H \in (0, \frac{3}{4}]$.

Now let us consider the numerator of (2.3). First we show that the eigenvalues of $C/\mathbb{E}\{S_j\}$ are bounded. By the Gershgorin circle Theorem, the eigenvalue corresponding to a row is not different from the corresponding diagonal element by more than the sum of the other elements in the row, i.e.,

$$|\tilde{\lambda}_i - 1| \leq \sum_{n \neq i} |C_{in}|/C_{11}, \quad \text{where} \quad C_{11} = \mathbb{E}\{S_j^2\}. \quad (17)$$

Since $\rho(k)$ decays as k^{2p-2H} , the sum in (17) approaches a constant in the limit as $N_j \rightarrow \infty$ for any H if the wavelet has at least two vanishing moments. Therefore

$$\lambda_i \leq K,$$

for some constant $K \geq 1$ independent of N_j . (Note that $\lambda_i > 0$.) Thus

$$\sum_{i=1}^{N_j} \lambda_i^3 \leq N_j K^3.$$

Hence, in the limit, J in (2.3) is given by

$$J = \frac{(2K^2/l(H))^{3/2}}{\sqrt{N_j}},$$

and goes to zero. From the Berry-Essen Theorem we conclude that

$$\frac{X_j}{\sqrt{l(H)}} = \frac{\sum_{i=1}^{N_j} \tilde{\lambda}_i (\xi_i^2 - 1)}{\sqrt{l(H)N_j}}$$

tends to a $\mathcal{N}(0,1)$ random variable in distribution. Thus, asymptotically, S_j is given by

$$S_j \stackrel{d}{=} \mathbb{E}\{S_j\} \left(1 + \epsilon_j \sqrt{\frac{l(H)}{N_j}} \right),$$

where ϵ_j is $\mathcal{N}(0, 1)$.

One can also show that the S_j 's are asymptotically jointly normal, by showing that $\sum_j a_j S_j$ is asymptotically normal for any $(a_j)_{1 \leq j \leq M}$ (where M is the number of scales) using the same line of argument as above. From the variance of the above sum one can find an expression for the asymptotic normalized covariance of (S_j) :

$$D_{j,i} = \frac{\text{Cov}(S_j, S_i)}{\mathbb{E}\{S_j\}\mathbb{E}\{S_i\}} \underset{N \rightarrow \infty}{\sim} \frac{1}{\sqrt{N_j N_i}} \quad (18)$$

where N_i is the number of detail coefficients at scale i , and N is the total number of data points. The asymptotic distribution of $\log_2(S_j)$ can be derived exactly the same way as in [36] for the pure fBm case, with Haar wavelets as the analyzing wavelets; therefore we will not repeat this analysis here. The distribution of $\log_2(S_j)$ is given by

$$\log_2(S_j) \stackrel{d}{=} \log_2(\mathbb{E}\{S_j\}) + \epsilon_j \sqrt{\frac{l(H)}{N_j \ln(2)}},$$

where ϵ_j is $\mathcal{N}(0, 1)$. □

In view of Theorem (2.1) we can use the generalized least squares estimate to estimate the Hurst parameter. If we denote $c := \log_2(\sigma^2 K(H))$, and $h := 2H + 1$ then the generalized least squares estimate of $b = [c, h]^T$ is given by

$$\tilde{b} = (X^T D^{-1} X)^{-1} X^T D^{-1} M \quad (19)$$

where $M = [\log_2(S_1), \dots, \log_2(S_J)]^T$, ($J = \log_2(N)$), D is given by (18), and X is given by

$$X = \begin{bmatrix} 1 & 1 \\ 1 & 2 \\ \vdots & \vdots \\ 1 & J \end{bmatrix}$$

We have

$$\begin{aligned} \mathbb{E}\{\tilde{c}\} &= \log_2(\sigma^2 K(H)), \\ \mathbb{E}\{\tilde{h}\} &= 2H + 1, \end{aligned}$$

and

$$\mathbb{E}\{\tilde{b}\tilde{b}^T\} = (X^T D^{-1} X \ln(2)^2)^{-1} \sim \frac{1}{N}$$

for large N . In view of these we have the following estimator for the Hurst parameter:

$$\tilde{H} = (\tilde{h} - 1)/2, \quad (20)$$

with variance

$$\text{Var}(\tilde{H}) \sim 1/(4N) \quad (21)$$

for large N .

In the next section we will allow σ in (8) to be stochastic. In particular we take σ to be any stochastic process having sufficient regularity.

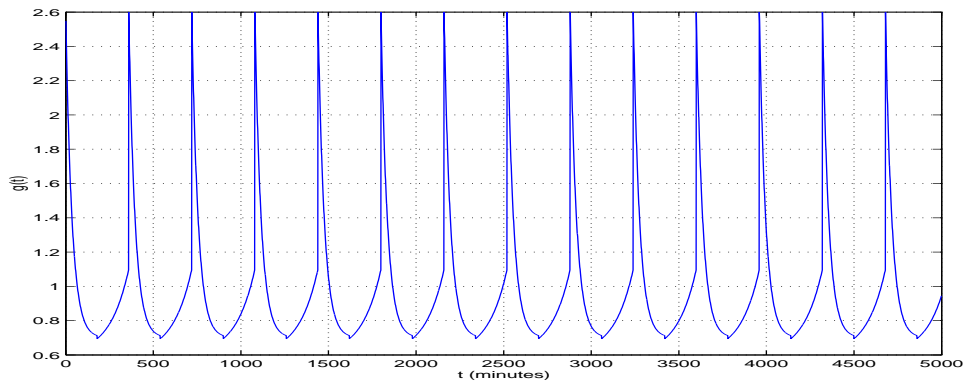


Figure 4: The periodic function g estimated from the S&P 500, whose one period is a good representative of the intraday variability of the index.

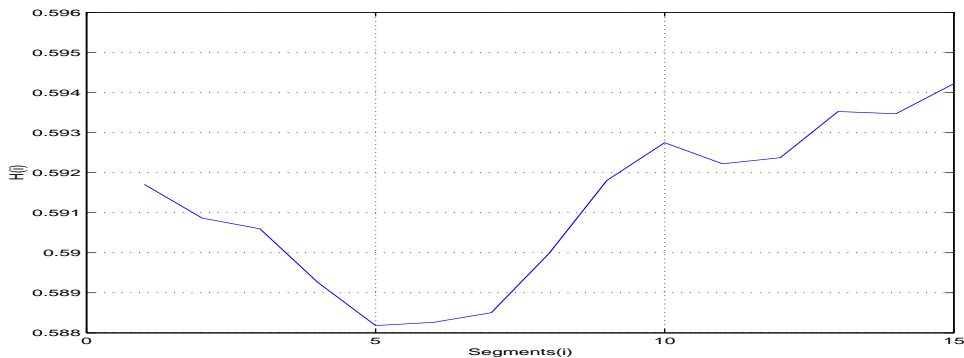


Figure 5: Hurst estimates from simulated data for (1) with $g(x)$ from Fig. 4, and with segments of length 2^{15} .

2.4 Robustness to Seasonalities and Volatility Persistence

We first present an empirical verification of robustness to seasonalities which is followed by a theoretical verification of robustness both to seasonalities and to volatility persistence.

We will denote the seasonal component with $g(x)$, where $x > 0$ is the time from the beginning of the segment under discussion. (Since the seasonal component is deterministic, we will denote it by $g(t)$ instead of σ_t to avoid confusion.) In examples such as $g(x) = (x + b)^q$, b denotes the beginning of the segment.

When (1) is implemented with a periodic g given by Fig. 4, which represents actual intraday variability, then the Hurst estimates do not change significantly. (The intraday variability envelope g of Fig. 4 was estimated from the S&P 500 index data as in [22].) The Hurst estimates also do not change when the amplitude of this periodic component is changed by a factor of 100. Estimates of the Hurst parameter for segments of length 2^{15} are shown in Fig. 5. (Compare with Fig. 2.2). The mean of the estimates over the segments is 0.5912, and the standard deviation is 0.0020.

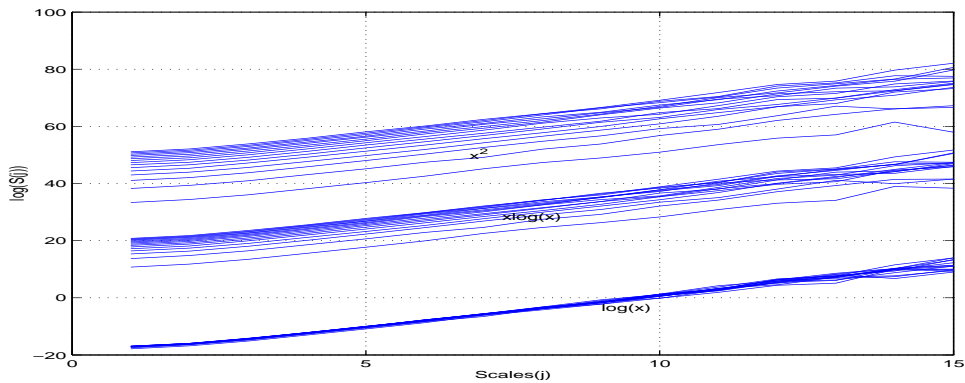


Figure 6: The log-scale spectrum for (1) with $g(x) = \log(x + b)$, $g(x) = (x + b)\log(x + b)$ and $g(x) = (x + b)^2$.

The scale spectra of (1) corresponding to various g 's, namely $g(x) = \log(x + b)$, $g(x) = (x + b)\log(x + b)$, $g(x) = (x + b)^2$, are plotted together on the same graph for comparison (Fig. 6). One immediately notices that the slope of the scale spectrum is invariant to the choice of g for these examples; only the amplitude changes with g . For the realization of fBm shown in Fig. 1, the mean and the std. for this parameter (over the segments) are: 0.5930, 0.0088; 0.5942, 0.0642; and 0.5953, 0.0062 for $g(x) = \log(x + b)$, $g(x) = (x + b)\log(x + b)$, and $g(x) = (x + b)^2$ respectively.

Path properties play an important role in the robustness of the estimator developed in the previous section in the case of stochastic volatility. First note that paths of B^H are almost surely Hölder continuous of order λ for all $\lambda < H$, due to the Kolmogorov-Čentsov Theorem ([26]).

The following result due to Ruzmaikina [41] and Zähle [48] gives the path properties of the stochastic integrals of a certain class of processes with respect to fBm.

Lemma 2.2 *Suppose σ is a stochastic process with almost surely Hölder continuous paths of order $\gamma > 1 - H$ on the interval $[0, T]$. Then the integral*

$$I_t = \int_0^t \sigma_s dB_s^H \quad (22)$$

exists almost surely as a limit of Riemann-Stieltjes sums. Furthermore, the process I is almost surely β -Hölder continuous on $[0, T]$ for any $\beta < H$.

Note that σ does not have to be adapted with respect to the natural filtration of B^H . For $H > 1/2$ an example of σ satisfying the conditions of Lemma 2.2 is the Wiener process. Any continuous periodic function also satisfies the assumptions of this theorem. (This is a rather straightforward example, but we cite it due to its relevance to seasonality issue.)

The following lemma is the key result for robustness; it gives a bound on the wavelet detail coefficients (9) for functions with certain regularity.

Lemma 2.3 *(See [28]) A function f is Hölder continuous of order γ if and only if the scale coefficients corresponding to f satisfy*

$$|d_j(k)| \leq A2^{j(\gamma+1/2)}, \quad \forall (j, k) \in \mathbb{Z}^2,$$

for some $A < \infty$.

The Hölder continuity exponent of a function is related to its finer scales; therefore one must use the scale coefficients defined in (9) for $j < 0$. Using Lemma 2.3 we have the following result.

Lemma 2.4 *Suppose f is a function that is Hölder continuous of order $\lambda < H$ and S_j is its scale spectrum. Then*

$$S_j \leq C_\gamma 2^{j(2\gamma+1)}, \quad \forall j \in \mathbb{Z}, \quad \forall \gamma < H, \quad (23)$$

for some $C_\gamma \in (0, \infty)$ and moreover (23) does not hold for $\gamma \geq H$ for infinitely many $j \in \mathbb{Z}_-$

and

$$\liminf_{j \rightarrow -\infty} \frac{\log(S_j)}{j} = 2H + 1.$$

Let us summarize the results of this section in the following theorem.

Theorem 2.2 *Suppose σ is a stochastic process with almost surely Hölder continuous paths of order $\gamma > 1 - H$ on the interval $[0, T]$. Then there exists a random variable $C_\gamma(\omega) \in (0, \infty)$ such that the scale spectrum of the integral (22) satisfies*

$$S_j(\omega) \leq C_\gamma(\omega) 2^{j(2\gamma+1)}, \quad \forall j \in \mathbb{Z}, \quad \forall \gamma < H, \quad (24)$$

almost surely. Moreover (24) almost surely does not hold for $\gamma > H$ for infinitely many $j \in \mathbb{Z}_-$ and

$$\liminf_{j \rightarrow -\infty} \frac{\log(S_j(\omega))}{j} = 2H + 1,$$

almost surely.

In Section 2.3, the domain of the wavelet is taken to be on the order of the mesh size of the discrete samples of the data. However the sample path properties show themselves in the finer detail coefficients ($j < 0$ in (9)). Then, using the fact that for any function f that is λ -Hölder continuous, $g(t) = f(at)$ is also λ -Hölder continuous, it can be seen that a scale spectrum for the finer scales can be obtained from a scale spectrum corresponding to coarser scales. Letting $J = \log_2(N) + 1$, where N is as in (10), we define $\psi'(t) = 2^{-J/2}\psi(at/2^J)$. Then ψ' is a wavelet which has the same number of vanishing moments as ψ . Taking $a = 1$, and defining the scale coefficients as

$$d'_j(k) := 2^{-j/2} \int_{-\infty}^{+\infty} \psi'(2^{-j}t - k)Z(t)dt, \quad j \in \mathbb{Z}_-$$

and scale spectrum as

$$S'_j := \frac{1}{N/2^j} \sum_{k=1}^{N/2^j} [d'_j(k)]^2 \quad j \in \mathbb{Z}_-$$

we have $S'_j = S_{J+j}$. So as the number of samples of the data increases ($J \rightarrow \infty$), we can consider finer and finer detail coefficients and the corresponding scale spectrum.

Since the log scale spectra corresponding to the synthetically constructed data for various kinds of seasonalities (see Fig. 6) and corresponding to the real data were linear, from Theorem

2.2 we can conclude that a linear regression is an accurate way of estimating the Hölder continuity exponent H of a sample path. This technique has been employed by Arneodo [6] for estimating the multifractal spectrum of a given sample path. (Also see [28]). Since the estimator given by (19) and (20) is a linear weighted least squares fit to the scale spectrum (giving more weight to the smaller scales, the weighting factor being proportional to the number of scale coefficients at the given scale) it is equal to the multifractal spectrum estimator of Arneodo.

3 Hurst Parameter Estimation for the S&P 500

After segmenting the samples of $\log(P_t/P_0)$ from our S&P 500 data set into dyadic segments, we estimated the Hurst parameter for each of the segments using the estimator given by (20). (Note that N is the number of points in a given segment.)

For each segment (20) requires computing the scale spectrum (10) which further requires the computation of the detail coefficients (9) for every scale. It may seem that this is computationally expensive for high frequency data; however due to the pyramidal algorithm described in Section A.1.2, this is not an issue. The pyramidal algorithm calculates the wavelet coefficients for any number of scales using octave filter banks given the initial approximation coefficients. Therefore the detail coefficients need only be computed at the initial scale. The detail coefficients at higher scales are computed from these initial coefficients via the pyramidal algorithm, which uses only the approximate coefficients of the preceding scale for calculating the detail coefficients of the next scale.

In our model we want to introduce the flexibility of having a variation in H . If we further partition the segments into smaller segments of equal length and estimate the Hurst parameter for these smaller segments, we expect to see noise in our estimates due to the noise introduced by making the segmentation length smaller. To be able to make a comparison between the Hurst estimates corresponding to different segmentation levels we must filter out the extra noise introduced. The following section introduces a method to remove this finite segmentation noise.

3.1 Filtering the Finite Segmentation Noise

We know that the log-scale spectrum method yields an asymptotically efficient estimator, and thus having smaller segment lengths will introduce noise into the estimates. To deal with the noise due to finite segmentation length, we will follow the approach of Papanicolaou and Solna [36], which we now review.

On letting \hat{h}^i denote the slope of the log-scale spectrum for the i th segment, we model it as

$$\hat{h}^i = h^i + \zeta^i,$$

where h^i is the true slope for the i th segment ($h^i = 2H^i + 1$), and ζ^i is a random variable that models the finiteness of the segments. The error term will be assumed to have zero mean, and for different segments the error terms will be assumed to be uncorrelated, i.e.

$$\mathbb{E}\{\zeta^i \zeta^j\} = 0, \quad i \neq j.$$

Here it is assumed that (H^i) is a stationary stochastic process independent of the fBm. On assuming that the slope process is exponentially correlated, l_h denotes its correlation length,

and σ_h^2 denotes its variance, we have

$$C_p(i, j) = \mathbb{E}\{(h^i - \mathbb{E}\{h^i\})(h^j - \mathbb{E}\{h^j\})\} = \sigma_h^2 \exp(-L|i - j|/l_h)$$

where L is the segment length.

Here we will give a minimum variance unbiased linear estimator for the slope process (\hat{h}^i) . Let \hat{K} denote the vector whose components are the estimates (\hat{h}^i) , and let K denote the vector whose components are the corresponding realizations of the slope process (h^i) . We want to find a filter such that

$$\mathbb{E}\{\|\Gamma\hat{K} - K\|^2\}$$

is minimized under the constraint that the mean is preserved, i.e.,

$$\Gamma\mathbb{E}\{K\} = \mathbb{E}\{K\}.$$

It can be shown that Γ is given by

$$\Gamma = (C_h + C_\zeta)^{-1}[C_h + u^T \otimes \mathbb{E}\{K\}], \quad (25)$$

where the vector $u = (u_i)$ is given by

$$u_i = \frac{\mathbb{E}\{h^i\} - \mathbb{E}\{K^T\}(C_h + C_\zeta)^{-1}C_{h,i}}{\mathbb{E}\{K^T\}(C_h + C_\zeta)^{-1}\mathbb{E}\{K\}}$$

and C_ζ is the diagonal covariance matrix of the estimation errors ζ^i . Here $C_{h,i}$ denotes the i th column of C_h . To be able to implement Γ one must estimate σ_h^2 and l_h of (3.1), and the variance σ_w^2 of the noise process. For this purpose we will examine the empirical variogram of the slope process (\hat{h}^i) . The variogram at lag j is given by

$$V(j) = \frac{1}{2(J-j)} \sum_{k=1}^{J-j} (\hat{h}^{k+j} - \hat{h}^k)^2$$

where J is the number of segments. Since

$$\mathbb{E}\{V(j)\} = \sigma_h^2(1 - \exp(-L|j|/l_h)) + \sigma_\zeta^2, \quad (26)$$

fitting (by a weighted least squares fit) the left-hand side of (26) to the empirical variogram yields the estimates for σ_h , σ_ζ and l_h . Here it should be noted that the initial values must be chosen carefully. The most important parameter seems to be the mean correlation length l_h , and we choose it to be longer than the segments used in estimating the slopes in order to have approximate stationarity relative to segmentation. Also note that it is necessary to perform a weighted fit to the empirical variogram, because there are finitely many segments, and therefore the empirical variogram is closer to its expected value for smaller lags.

We will now illustrate the power of filtering in removing the effects of noise due to finite segmentation length on one realization of the synthetically created fBm of Fig. 1. We partitioned the data into segments of length 2^{13} , estimated the Hurst parameter for each of the segments, and then applied filtering. (ΓP where Γ is given in (25).) The Hurst estimates we obtained with and without filtering are given in Fig. 7. The standard variation without filtering is 0.0283, and the standard variation after filtering is 0.0097; so clearly we mitigate to the finite segment length effects by filtering.

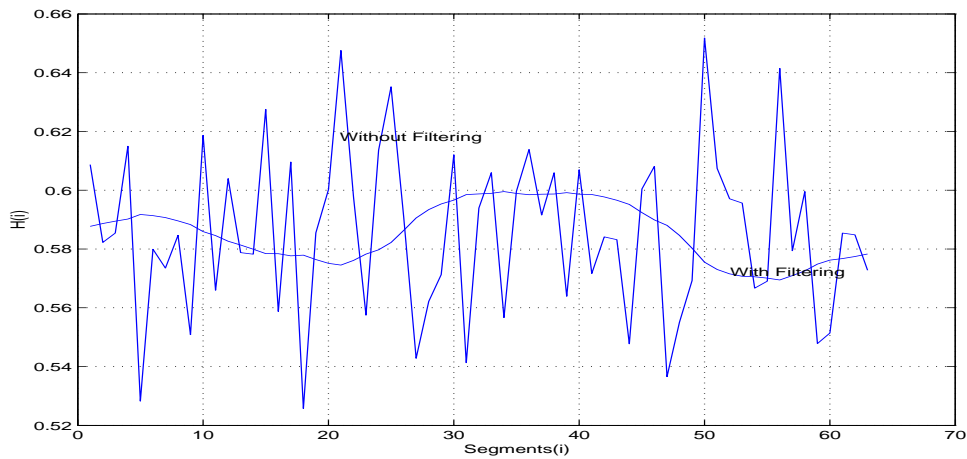


Figure 7: Hurst estimates for the realization given in Fig. 1 for 64 segments of length 2^{13} with and without filtering.

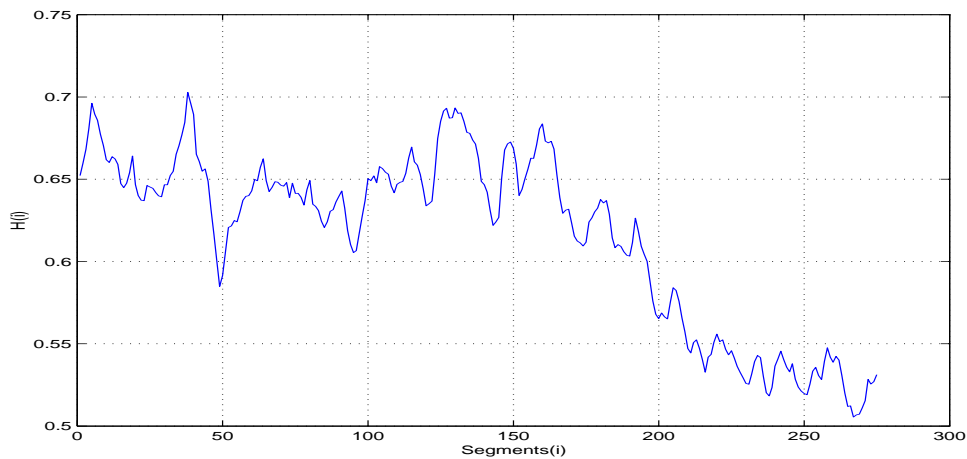


Figure 8: Hurst parameter estimates for the S&P 500 data with segment lengths of 2^{12}

3.2 Results on the S&P 500 Index

We now turn our attention to the analysis of the S&P 500 index. As noted above, we consider data taken at one-minute intervals over the course of 11.5 years from January 1989 to May 2000. (We take the closing price of each minute.) The data consists of 1,128,360 observations, which is on the order of 2^{20} .

When the data is segmented into 275 segments of length 2^{12} (approximately two weeks) and the above methodology is applied, we obtain the Hurst parameter estimates shown in Fig. 8. (The mean is 0.6156, and the standard deviation is 0.0531, which supports the idea of local variation, i.e. the Hurst parameter varies significantly from segment to segment.)

Alternatively, when the data is segmented into 137 segments of length 2^{13} (approximately four weeks), we obtain the Hurst parameter estimates shown in Fig. 9. (The mean is 0.6027, and the std. is 0.0504.)

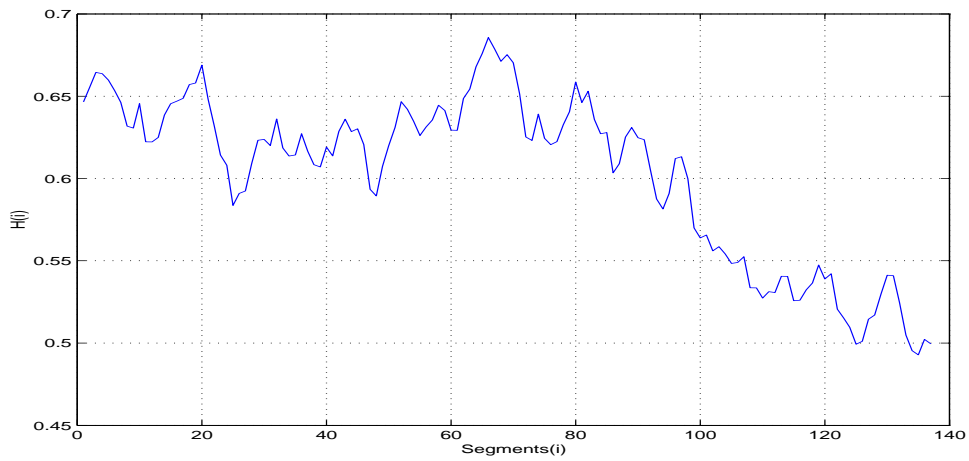


Figure 9: Hurst parameter estimates for the S&P 500 data with segment lengths of 2^{13}

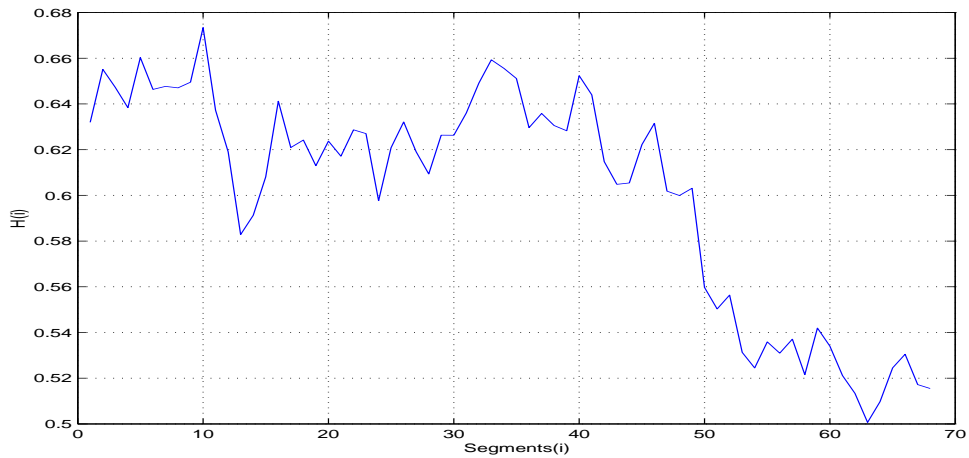


Figure 10: Hurst parameter estimates for the S&P 500 data with segment lengths of 2^{14}

Similarly, when the data is segmented into 68 segments of length 2^{14} (approximately four weeks), we obtain the Hurst parameter estimates shown in Fig. 10. (The mean is 0.6011 and the std. is 0.0487.) And, finally, when the data is segmented into 34 segments of length 2^{15} (approximately eight weeks), we obtain the Hurst parameter estimates given in Fig. 11. (The mean is 0.6008 and the std. is 0.1821.)

If we plot these results on the same axes as shown in Fig. 12 we will arrive at the significant observation that the length of a stationary segment is 2^{14} , which corresponds to approximately 2 months. That is, when the segments are of length 2^{15} , the nonstationarity is dominant.

3.3 Increase in the Market Efficiency

From Fig. 10, one sees that, although the Hurst parameter of this data set is significantly above the efficient markets value of $H = \frac{1}{2}$, it began to approach that level in 1997 (segment 50). We

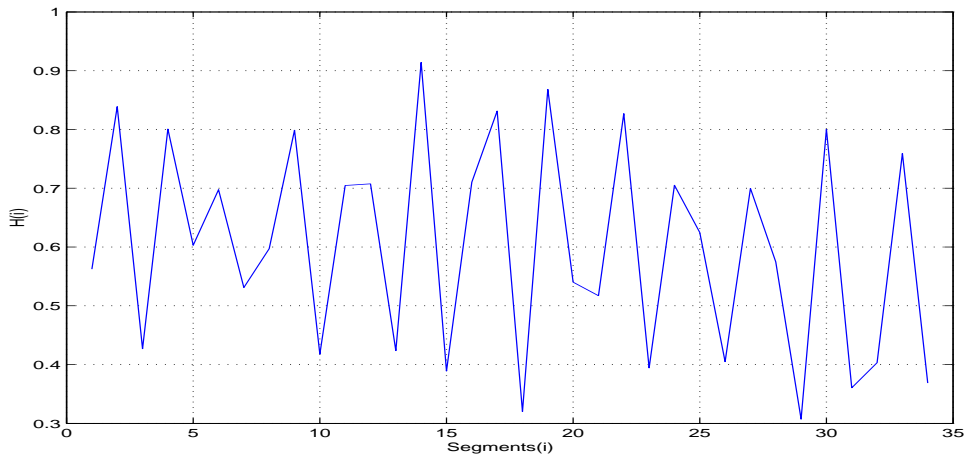


Figure 11: Hurst parameter estimates for the S&P 500 data with segment lengths of 2^{15}

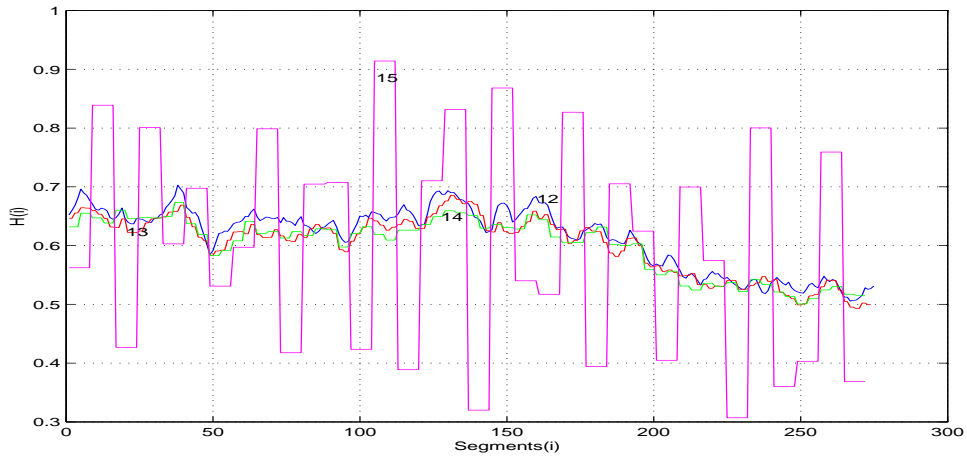


Figure 12: Hurst parameter estimates for the S&P 500 data with various segment lengths. The strongly varying graph corresponds to estimates for segment lengths of 2^{15} points. The graphs corresponding to the segment lengths of 2^{12} , 2^{13} , 2^{14} can be distinguished from the line intensity, where the intensity decreases as the segment length increases, moreover the graphs are labeled by \log_2 of the corresponding segments length.

conjecture that this behavior of the market might be related to the increase in Internet trading, which had the three-fold effect of increasing the number of small traders, the frequency of trading activity and the availability of market data. This observation is modeled in [10], with a simple microstructure model for the price evolution of a financial asset where the price is driven by the demand of many small investors whose trading behavior exhibits “inertia”. This means that the agents trade the asset infrequently and are inactive most of the time. It is shown that when the price process is driven by market imbalance, the logarithm of the price process is approximated by a process of the form (8). Moreover it is shown that as the frequency of trading increases, the price process can be approximated by geometric Brownian motion, which is consistent with the above comments.

4 Conclusion

In this paper we have developed a method to investigate long range dependence, which is quantified by the Hurst parameter, in high frequency financial time series. Our method exhibits robustness to the non-stationarities that are present in the data, e.g. seasonal volatility, fat-tailed distributions of the increments, and possible variations in the Hurst parameter. (In fact, the Hurst parameter reflects the relative frequency of the trading activity of the market participants, and hence variations in the Hurst parameter are expected [10].) The segments of stationarity for the Hurst parameter are byproducts of this analysis. They are found to be approximately two months in duration for S&P 500 index data sampled at one minute intervals. Strikingly, the Hurst parameter was around the 0.6 level for most of the 1990s, but dropped closer to the efficient markets level of 0.5 in the period 1997-2000, coinciding with the growth in Internet trading among small investors.

A Appendix

A.1 Wavelet Theory

For a more detailed treatment see [17], [28] or [34].

A.1.1 Multi-resolution Analysis

A wavelet ψ is a function mapping \mathbb{R} to \mathbb{R} such that the dilated and translated family

$$\psi_{j,k}(t) = 2^{-j/2}\psi(2^{-j}t - k) \quad \text{for } (j, k) \in \mathbb{Z}^2,$$

is an orthonormal basis of $L^2(\mathbb{R})$. A wavelet is defined via a *scaling function* through multi-resolution analysis (MRA). A sequence of closed subspaces $\{V_j, j \in \mathbb{Z}\}$ of $L^2(\mathbb{R})$ is an MRA if the following six properties are satisfied:

$$\begin{aligned} \bigcap_{j \in \mathbb{Z}} V_j &= \{0\}, \\ \text{Closure}\left(\bigcup_{j \in \mathbb{Z}} V_j\right) &= L^2(\mathbb{R}), \\ V_{j+1} &\subset V_j, \\ \forall (j, k) \in \mathbb{Z}^2, \quad f(t) \in V_j &\Leftrightarrow f(t - 2^j k) \in V_j, \\ \forall j \in \mathbb{Z}, \quad f(t) \in V_j &\Leftrightarrow f\left(\frac{t}{2}\right) \in V_{j+1}, \end{aligned}$$

and, there exists a function $\phi(t)$ in V_0 , called the scaling function, such that the collection

$$\{\phi(t - k), k \in \mathbb{Z}\}$$

is a Riesz basis for V_0 .

It follows that the scaled and shifted functions of the scaling function

$$\{\phi_{j,k}(t) = 2^{-j/2}\phi(2^{-j}t - k), k \in \mathbb{Z}\}$$

is an orthonormal basis of V_j for all j .

Orthonormal wavelets carry the details necessary to increase the resolution of a signal approximation. The approximations of a function $f \in L^2(\mathbb{R})$ at scales 2^j and 2^{j-1} are respectively equal to its orthogonal projections onto V_j and V_{j-1} . Let W_j be the orthogonal complement of V_j in V_{j-1} , *i.e.* $V_{j-1} = V_j \oplus W_j$. Then the orthogonal projection of f onto V_{j-1} can be decomposed as the sum of orthogonal projections onto V_j and W_j . The projection onto W_j provides the *details* that appear at scale 2^{j-1} but which disappear at the coarser scale 2^j . One can construct an orthonormal basis of W_j by scaling and translating a wavelet $\psi \in V_0$, and show that the family given by (A.1.1) is an orthonormal basis for $L^2(\mathbb{R})$. Since ψ and ϕ are in V_0 , and by the properties of MRA we have:

$$\phi(t) = \sqrt{2} \sum_{k=0}^M h(k) \phi(2t - k),$$

and

$$\psi(t) = \sqrt{2} \sum_{k=0}^M g(k) \phi(2t - k),$$

where h is a low-pass filter satisfying some admissibility conditions (see [28]), and g is the conjugate mirror filter of h :

$$g(n) = (-1)^{1-n} h(1 - n).$$

Therefore wavelets are specified via the scaling filter h .

Wavelets are capable of removing nonstationarities because they have vanishing moments. We say that ψ has p vanishing moments if it is orthogonal to any polynomial of degree less than p :

$$\int_{-\infty}^{+\infty} t^k \psi(t) dt = 0 \quad \text{for} \quad 0 \leq k < p. \quad (27)$$

The most versatile wavelet family is the family of Daubechies compactly supported wavelets, which are enumerated by their number of vanishing moments. The Daubechies compactly supported wavelet with $p = 1$ is the Haar wavelet, which is the only wavelet in this family for which an explicit expression can be found. In our analysis we used Daubechies compactly supported wavelets with $p = 2$.

A.1.2 Pyramidal Algorithm (Mallat Algorithm) and its Initialization

Let us denote the projection of a function $f \in L^2(\mathbb{R})$ onto V_j and W_j respectively by

$$a_j(k) = \langle f, \phi_{j,k} \rangle \quad \text{and} \quad d_j(k) = \langle f, \psi_{j,k} \rangle, \quad k \in \mathbb{Z},$$

where $\langle \cdot, \cdot \rangle$ denotes the standard L^2 inner product. The pyramidal algorithm calculates these coefficients efficiently with a cascade of discrete convolutions and subsamplings. Denote time reversal by $\bar{x}(n) = x(-n)$ and upsampling by

$$\check{x}(n) = \begin{cases} x(n) & \text{if } n \text{ is even,} \\ 0 & \text{if } n \text{ is odd.} \end{cases}$$

The pyramidal algorithm is then given by the following theorem:

Theorem A.1 (Mallat [28]) *Decomposition:*

$$a_{j+1}(p) = \sum_{n=-\infty}^{+\infty} h(n-2p)a_j(n) = a_j \star \bar{h}(2p)$$

$$d_{j+1}(p) = \sum_{n=-\infty}^{+\infty} g(n-2p)a_j(n) = a_j \star \bar{g}(2p).$$

Reconstruction:

$$a_j(p) = \sum_{n=-\infty}^{+\infty} h(p-2n)a_{j+1}(n) + \sum_{n=-\infty}^{+\infty} g(p-2n)d_{j+1}(n)$$

$$= \check{a}_{j+1} \star h(p) + \check{d}_{j+1} \star g(p).$$

To compute the detail coefficient at scale j , we use only the approximation coefficient at the previous scale a_{j-1} . Note that the domain of h and g are compact if we use Daubechies wavelets with compact support.

The pyramidal algorithm assumes initially that it is given the wavelet coefficients at a fine scale, and proceeds to compute the detail coefficients at higher scales. The initial sequence $a_0(k)$ requires the evaluation of a continuous time integral,

$$a_0(k) = \int_{\mathbf{R}} f(t)\phi(t-k) dt, \quad (28)$$

where ϕ is the scaling function.

Typically what is done is to set $a_0(k) = f(k)$, an ad-hoc procedure that will almost certainly introduce errors. (An exception is the case in which *coiflets* [28] are used, since in that case the scaling function has vanishing moments of the same order as the wavelet.) Here, we will replace the continuous time integral by a sum:

$$a_0(k) = \sum_n f(n)\phi(n-k).$$

Note that this sum is equal to the integral of (28) when $f(t)$ is a low order polynomial. (See [34].) An explicit expression for ϕ is not known, however ϕ at the integer points can be calculated from the defining recursion for the scale function:

$$\phi(t) = \sqrt{2} \sum_{k=0}^M h(k)\phi(2t-k).$$

There are better methods one could apply for the initialization, as suggested by Beylkin *et al.* in [11].

Remark A.1 *We use only the vanishing moments property (27) and compactness of the support of the wavelets to prove Theorems 2.1 and 2.2. However we need the orthogonality introduced by the multiresolution analysis for implementing the pyramidal algorithm introduced in Section A.1.2. Moreover in our analysis of the S&P 500 index data we work with compactly supported wavelets to further increase the efficiency of the pyramidal algorithm.*

References

- [1] ABRY, P. , and D. VEITCH (1998): Wavelet Analysis of Long-range-dependent Traffic, *IEEE Transactions on Information Theory* 44, 2-15.
- [2] ABRY, P., and F. SELLAN (1996): The Wavelet-Based Synthesis for Fractional Brownian Motion Proposed by F. Sellan and Y. Meyer: Remarks and Fast Implementation, *Applied and Computational Harmonic Analysis* 3, 377-383
- [3] ANDERSEN, T. G. , and T. BOLLERSLEV (1997): Heterogeneous Information Arrivals and Return Volatility Dynamics: Uncovering the Long-Run in High Frequency Returns, *Journal of Finance* 52, 975-1005.
- [4] ANDERSEN, T. G. , and T. BOLLERSLEV (1997): Intraday Periodicity and Volatility Persistence in Financial Markets, *Journal of Empirical Finance* 4, 115-158
- [5] ANDERSEN, T. G. , and T. BOLLERSLEV (1998): Deutsche Mark-Dollar Volatility: Intraday Activity Patterns, Macroeconomic Announcements, and Longer Run Dependencies, *Journal of Finance* 53, 219-265.
- [6] ARNEODO, A. (1996): Wavelet Analysis of Fractals, *Wavelets: Theory and Applications*, Oxford University Press, New York.
- [7] BARUCCI, E., P. MALLIAVIN, M. E. MANCINO, R. RENO (2003): The Price-Volatility Feedback Rate: An Implementable Mathematical Indicator of Market Stability, *Mathematical Finance*, 13, 17-37.
- [8] BAYRAKTAR, E. and H. V. POOR (2001): Arbitrage in Fractal Modulated Markets When the Volatility is Stochastic, *preprint, Princeton University*.
- [9] BAYRAKTAR, E., H. V. POOR (2002): Stochastic Differential Games in a Non-Markovian Setting, *preprint, Princeton University*.
- [10] BAYRAKTAR, E., U. HORST, K. R. SIRCAR (2003) A Limit Theorem for Financial Markets with Inert Investors, *preprint, Princeton University*.
- [11] BEYLKIN, G., R. R. COIFMAN, and V. ROKHLIN (1992): Wavelets in Numerical Analysis, *Wavelets and Their Applications*, 181-210. Jones and Barlett.
- [12] BJÖRK, T. and H. HULT (2003): A Note on the Self-Financing Condition for the Fractional Black-Scholes Model, *preprint, University of Stockholm*.
- [13] BLACK, F. and M. SCHOLES (1973): The Pricing of Options and Corporate Liabilities, *J. Political Econ.*, 81, 637-659.
- [14] CHERIDITO, P. (2003): Arbitrage in Fractional Brownian Motion Models, *Finance and Stochastics*, 7, 533-553.
- [15] COX, J., S. ROSS, and M. RUBINSTEIN (1979): Option Pricing: A Simplified Approach, *J. Financial Economics* 7, 229-263
- [16] CUTLAND, N. J., P. E. KOPP, and W. WILLINGER (1995): Stock Price Returns and the Joseph Effect: A Fractal Version of the Black-Scholes model. *Progress in Probability* 36, 327-351.
- [17] DAUBECHIES, I. C. (1992): *Ten Lectures on Wavelets*, SIAM, Philadelphia.
- [18] DUNCAN, T. E., Y. HU AND B. PASIK-DUNCAN (2000): Stochastic Calculus for Fractional Brownian Motion, *SIAM Journal of Control and Optimization*, 38, 582-612.
- [19] ELLIOTT R. J. and J. VAN DER HOEK (2003): A General Fractional White Noise Theory and Applications to Finance, *Mathematical Finance*, 13, 301-330.
- [20] FAMA, E. F. (1965): The Behaviour of Stock Market Prices, *Journal of Business*, 38, 34-105.

- [21] GREENE, M. T. and B. D. FIELITZ (1977): Long-Term Dependence in Common Stock Returns, *Journal of Financial Economics*, 4, 339-349.
- [22] FOUQUE, J. P., G. PAPANICOLAOU, R. SIRCAR, and K. SOLNA(2003): Short Time-scale in S&P 500 Volatility, *Journal of Computational Finance*, 6(4), 1-23.
- [23] GENÇAY, R., F. SELÇUK, and B. WHITCHER (2001): Differentiating Intraday Seasonalities Through Wavelet Multi-Scaling *Physica A* 289, 543-556.
- [24] HALL, P., W. HÄRDLE, T. KLEINOW and P. SCHMIDT (2000): Semiparametric Bootstrap Approach To Hypothesis Tests And Confidence Intervals For The Hurst Coefficient, *Statistical Inference for Stochastic Processes*, 3, 263-276.
- [25] HIDA, T., H. KUO, J. POTHOFF and L. STREIT (1993): *White Noise, an Infinite Dimensional Calculus*, Kluwer Academic Publishers, Boston.
- [26] KARATZAS, I. and S.E. SHREVE (1991): *Brownian Motion and Stochastic Calculus*, Springer-Verlag, New York.
- [27] LO, A. W. (1991): Long-term Memory in Stock Market Prices, *Econometrica*, 59, 1279-1313.
- [28] MALLAT, S. (2001): *A Wavelet Tour of Signal Processing*, Academic Press, San Diego.
- [29] MANDELBROT, B. B. (1963): The Variation of Certain Speculative Prices, *The Journal of Business*, 36, 394-419.
- [30] MANDELBROT, B.B. (1967): Forecasts of Future Prices, Unbiased Markets and Martingale Models, *Journal of Business*, 39, 242-255.
- [31] MANDELBROT, B.B. (1971): When Can Price Be Arbitraged Efficiently? A Limit to the Validity of the Random Walk and Martingale Models, *Rev. Econom. Statis.*, 53, 225-236.
- [32] MANDELBROT, B. B. (1997): *Fractals and Scaling in Finance*, Springer-Verlag, New York.
- [33] MERTON, R. C. (1969): Lifetime Portfolio Selection Under Uncertainty: The Continuous-time Case, *Rev. Econom. Statist.* 51, 247-257.
- [34] NGUYEN T. and G. STRANG (1997): *Wavelets and Filter Banks*, Wellesley-Cambridge Press, Wellesley, MA.
- [35] ØKSENDAL, B. and Y. HU (2000): Fractional White Noise and Applications to Finance, *Infinite Dimensional Analysis, Quantum Probability and Related Topics*, 6, 1-32.
- [36] PAPANICOLAOU, G. and K. SOLNA (2001): Wavelet Based Estimation of Local Kolmogorov Turbulence, In 'Long-Range Dependence Theory and Applications', edited by P.Doukhan, G.Oppenheim, M.S. Taqqu, Birkhauser, Boston.
- [37] PETERS, E. E. (1991): *Chaos and Order in the Capital Markets*, John Wiley and Sons, New York.
- [38] PETERS, E. E (1994): *Fractal Market Analysis: Applying Chaos Theory to Investment and Economics*, John Wiley and Sons, New York.
- [39] PROTTER, P. (1990): *Stochastic Integration and Differential Equations*. Springer-Verlag, Berlin.
- [40] ROGERS, C. (1997): Arbitrage with fractional Brownian motion, *Mathematical Finance* 7, 95-105.
- [41] RUZMAIKINA, A. A. (1999): *Stochastic Calculus with Fractional Brownian Motion*, Ph.D Dissertation, Department of Physics, Princeton University, Princeton, NJ.
- [42] SAMORODNITSKY, G. and M. S. TAQQU (1994): *Stable Non-Gaussian Random Processes*, Chapman & Hall, London.
- [43] SHIRYAEV, A. N. (1999): *Essentials of Stochastic Finance*. World Scientific, Singapore.
- [44] SOTTINEN, T. and E. VALKEILA (2003): On arbitrage and replication in the fractional Black-Scholes pricing model, *Statistics and Decisions*, 21, 93-107.

- [45] STROOCK, D. W.(1993): *Probability Theory*, Cambridge University Press, Cambridge UK.
- [46] TEVEROVSKY, V., M. S. TAQQU and W. WILLINGER (1999): A Critical Look at Lo's Modified R/S Statistic, *Journal of Statistical Planning and Inference*, 80, 211-227.
- [47] WILLINGER, W., M. S. TAQQU and V. TEVEROVSKY (1999): Stock Market Prices and Long-range Dependence, *Finance and Stochastics*, 3, 1-13.
- [48] ZÄHLE, M. (1998): Integration with Respect to Fractal Functions and Stochastic Calculus. I, *Probability Theory and Related Fields*, 111, 333-374.